



LAWRENCE  
LIVERMORE  
NATIONAL  
LABORATORY

# Synthesis and Performance Characterization of a Nanocomposite Ternary Thermite: Al/Fe<sub>2</sub>O<sub>3</sub>/SiO<sub>2</sub>

D. Prentice, M. L. Pantoya, B. J. Clapsaddle

February 7, 2005

JOURNAL OF PHYSICAL CHEMISTRY B

## **Disclaimer**

---

This document was prepared as an account of work sponsored by an agency of the United States Government. Neither the United States Government nor the University of California nor any of their employees, makes any warranty, express or implied, or assumes any legal liability or responsibility for the accuracy, completeness, or usefulness of any information, apparatus, product, or process disclosed, or represents that its use would not infringe privately owned rights. Reference herein to any specific commercial product, process, or service by trade name, trademark, manufacturer, or otherwise, does not necessarily constitute or imply its endorsement, recommendation, or favoring by the United States Government or the University of California. The views and opinions of authors expressed herein do not necessarily state or reflect those of the United States Government or the University of California, and shall not be used for advertising or product endorsement purposes.

# Synthesis and Performance Characterization of a Nanocomposite Ternary Thermite: Al/Fe<sub>2</sub>O<sub>3</sub>/SiO<sub>2</sub>\*\*

By *Daniel Prentice, Michelle L. Pantoya, and Brady Clapsaddle\**

Making solid energetic materials requires the physical mixing of solid fuels and oxidizers or the incorporation of fuel and oxidizing moieties into a single molecule. The former are referred to as composite energetic materials (i.e., thermites, propellants, pyrotechnics) and the latter are deemed monomolecular energetic materials (i.e., explosives). Mass diffusion between the fuel and oxidizer is the rate controlling step for composite reactions while bond breaking and chemical kinetics control monomolecular reactions. Although composites have higher energy densities than monomolecular species, they release that energy over a longer period of time because diffusion controlled reactions are considerably slower than chemistry controlled reactions. Conversely, monomolecular species exhibit greater power due to more rapid kinetics than physically mixed energetics.

Reducing the diffusion distance between fuel and oxidizer species within an energetic composite would enhance the reaction rate.<sup>[1,2]</sup> Recent advances in nanotechnology have spurred the development of nano-scale fuel and oxidizer particles that can be combined into a composite and effectively reduce diffusion distances to nano-scale dimensions or less.<sup>[2,3]</sup> These

---

[\*] Prof. M. L. Pantoya  
Department of Mechanical Engineering  
Corner of 7<sup>th</sup> and Boston Ave.  
Texas Tech University  
Lubbock, TX 79409 (U.S.A.)  
E-mail: michelle.pantoya@coe.ttu.edu

Dr. B. J. Clapsaddle  
Chemistry and Materials Science Directorate and Energetic Materials Center  
Lawrence Livermore National Laboratory  
7000 East Avenue, L-092  
Livermore, CA 94550 (U.S.A.)  
E-mail: clapsaddle1@llnl.gov

[\*\*] The authors gratefully acknowledge support from the Army Research Office (Contract Number DAAD19-02-1-0214). Some of this work was done under the auspices of the U.S. Department of Energy by the University of California, Lawrence Livermore Laboratory under contract No. W-7405-Eng-48.

nanocomposites have the potential to deliver the best of both worlds: high energy density of the physically mixed composite with the high power of the monomolecular species. Toward this end, researchers at Lawrence Livermore National Laboratory (LLNL) developed nano-particle synthesis techniques, based on sol-gel chemistry, for the production of thermite nanocomposites.<sup>[4]</sup> Thermite reactions are traditionally fuel and oxidizer powders that are mixed to make an energetic material based on the general oxidation reaction shown in Equation 1,



where  $M^1$  is a fuel, such as aluminum metal, and  $M^2O_x$  is a metal oxide, such as  $Fe_2O_3$ .

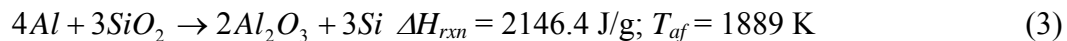
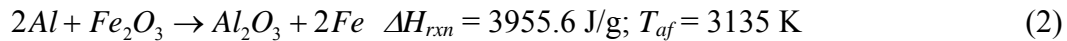
Recently, Plantier *et al.* showed that the oxidizer synthesis technique is a strong function of the combustion behavior of the composite.<sup>[5]</sup> In that study,  $Fe_2O_3$  was synthesized using sol-gel chemistry to create a high surface area, nano-particulate  $Fe_2O_3$  aerogel powder and a lower surface area, nano-particulate  $Fe_2O_3$  xerogel powder. The combustion velocities of these two oxidizers mixed with nano-scale Al particles were examined and compared to a commercially obtained nano-particulate  $Fe_2O_3$  powder combined with the same nano-scale Al particles. The results showed that the combustion velocity ranged from 1 to 900 m/s, and the sol-gel derived, aerogel  $Fe_2O_3$  outperformed all other oxide powders. The results also showed that a reaction can be tailored to a specific application by controlling the synthesis process.

More recently, Clapsaddle *et al.* developed a generalized method for the synthesis of metal oxide-silicon oxide nanocomposites with the metal oxide as the major phase.<sup>[4c,4d]</sup> They applied this method to construct the first  $Fe_2O_3$ - $SiO_2$  mixed oxide nanocomposites with the iron (III) oxide as the major component. The resulting aerogel and xerogel nanocomposites showed a high degree of dispersion between the  $Fe_2O_3$  and the  $SiO_2$  on the nanoscale.<sup>[4c]</sup> These nanocomposite aerogel oxidizers have recently been shown to be of use in energetic

applications.<sup>[6,7]</sup> Such a composite requires that a more energetic metal oxide, such as Fe<sub>2</sub>O<sub>3</sub>, be the major phase in order to produce an exothermic reaction when the metal-oxide is combined with a fuel such as aluminum. The motivation for including a less energetic metal oxide, such as SiO<sub>2</sub>, is to tailor the energy release properties to a specific application by changing the chemical and physical properties of the oxidizer.

The goal of this work is to examine the influence of SiO<sub>2</sub> on the energy release properties of the Al/Fe<sub>2</sub>O<sub>3</sub> thermite reaction. This objective was accomplished by comparing the combustion velocities of two separate Al-Fe<sub>2</sub>O<sub>3</sub>-SiO<sub>2</sub> nanocomposites: one prepared from commercially obtained individual nano-scale particles; and, the other prepared by combining nano-scale Al with sol-gel synthesized Fe<sub>2</sub>O<sub>3</sub>-SiO<sub>2</sub> aerogel nanocomposites. In the case of the latter, aerogel powders were chosen due to their superior combustion velocities as demonstrated by Plantier *et. al.*<sup>[5]</sup>

Previous work showed that an Al/Fe<sub>2</sub>O<sub>3</sub> composite burns at an optimum equivalence ratio ( $\Phi$ ) equal to 1.2 corresponding to a slightly fuel-rich mixture.<sup>[5]</sup> This composition is also consistent with the optimum combustion behavior of many other thermites and was selected as the composition for these experiments.<sup>[8]</sup> To calculate the correct proportions of each reactant component according to an equivalence ratio of 1.2, the stoichiometric reactions are needed. Equations 2 and 3 show the stoichiometric reactions between Al and Fe<sub>2</sub>O<sub>3</sub> and Al and SiO<sub>2</sub> and the corresponding heats of reaction ( $\Delta H_{rxn}$ ) and adiabatic flame temperature ( $T_{af}$ ).<sup>[9]</sup>



Based on these reactions, the stoichiometric (*st*) fuel/oxidizer ratios are shown in Equations 4 and 5.

$$\left(\frac{Fuel}{Ox}\right)_{st, Fe_2O_3} = 0.338 \quad (4)$$

$$\left(\frac{Fuel}{Ox}\right)_{st, SiO_2} = 0.599 \quad (5)$$

To calculate the total stoichiometric fuel/oxidizer ratio for the combined reaction, a weighted average was determined from a specified mass percent oxidizer composition of  $Fe_2O_3$  and  $SiO_2$ . Six combinations of oxidizers were prepared ranging from 100 %  $Fe_2O_3$  and 0 %  $SiO_2$  to 0 %  $Fe_2O_3$  and 100 %  $SiO_2$  in 20 % increments as shown in Fig. 1.

Equation 6 shows the calculation of the actual fuel/oxidizer ratio based on the stoichiometric ratios (Equations 4 and 5) and an  $\Phi = 1.2$ .

$$\left(\frac{Fuel}{Ox}\right)_{actual} = \Phi * \left(\frac{Fuel}{Ox}\right)_{st, total} \quad (6)$$

Equation 7 shows the calculation of the mass percent fuel for the each composition and Equation 8 shows the calculation of the mass percent oxidizer.

$$\left(\frac{Fuel}{Ox}\right)_{actual} = \frac{(\% mass Al) * (\% active Al content)}{(1 - \% mass Al)} \quad (7)$$

$$(1 - \% mass Al) = \% mass Ox \quad (8)$$

Equations 9 and 10 show the calculations of the mass percent of  $Fe_2O_3$  and  $SiO_2$ .

$$(\% mass Fe_2O_3)_{composite} = (\% mass Ox) * (\% mass Fe_2O_3)_{oxidizer} \quad (9)$$

$$(\% mass SiO_2)_{composite} = (\% mass Ox) * (\% mass SiO_2)_{oxidizer} \quad (10)$$

The composite subscripts denote the total mass percent of the specific component and the oxidizer subscript denotes only the mass percent found in the oxidizer itself. For example, an oxidizer with 20% mass  $Fe_2O_3$  and 80% mass  $SiO_2$  would have 11.1 % mass  $Fe_2O_3$  and 44.3 % mass  $SiO_2$  in relation to the total mixed composite at  $\Phi=1.2$ . Also, the previous example would

have 44.7 % mass Al. Furthermore the amount of Al fuel metal for each mixture varies by no more than 10% over the entire series.

Using the calculated ratios described above, two sets of energetic powders were produced, each containing binary  $\text{Fe}_2\text{O}_3/\text{SiO}_2$  oxidizing phases. The first set was prepared by physically mixing commercial nm Al powder with an aerogel oxidizer composite in which the  $\text{Fe}_2\text{O}_3$  and  $\text{SiO}_2$  components were simultaneously generated in situ using sol-gel chemistry. The oxidizer composite in this mixture will be referred to as *Oxidizer A* and the fuel/oxidizer composite will be referred to as *Thermite A*. The second set consisted of commercially available nano-scale particles of  $\text{Fe}_2\text{O}_3$  and  $\text{SiO}_2$  that are combined with the same commercial nm Al powder through mechanical mixing using an ultrasonification process. This mixture contains discrete particles of  $\text{Fe}_2\text{O}_3$  and  $\text{SiO}_2$  as the oxidizer and will be referred to as *Oxidizer B*, and the fuel/oxidizer composite will be referred to as *Thermite B*. In this way, the effect of sol-gel synthesis on the oxidizer can be isolated with respect to the entire composite. A summary of oxidizing phase compositions for both the sol-gel (*Oxidizer A*) and mechanically prepared (*Oxidizer B*) composites is shown in Figure 1. The same weighted percentage method of calculating a total fuel/oxidizer ratio was applied to the aerogel oxidizers by using the oxidizer elemental analysis data shown in Table 1. With the exception of the use of Equations 9 and 10, which are unnecessary in the case of the aerogel oxidizers, the same mixing procedure was used for both sets of thermite composites (*Thermite A and B*).

For this study characterizing the energetic performance involved measuring the combustion velocity. There are several different experimental configurations that can be employed to measure and quantify combustion velocity. Some include examining flame propagation in loose powders either confined within a tube<sup>[5, 10]</sup> or open to the environment.<sup>[5]</sup> For

this analysis, flame propagation was examined for loose powders in a channel open to an air environment. Figure 2 is a photograph of the transparent acrylic block burning apparatus. In this configuration, the powder is confined on three sides by the channel but open to an ambient air environment on the top. Although the amount of material and the volume of the channel are controlled, density gradients may still exist along the sample length. Care was taken to ensure homogeneity in the quality of the sample.

Figure 3 shows the combustion velocity as a function of weight percent  $\text{SiO}_2$  content and as a function of the oxidizer synthesis technique. Each data symbol represents an average measurement from 3 or 4 experiments. The standard deviations in measurements are  $\pm 0.001$  m/s and thus the error bars associated with each data symbol are too small to appear in Fig. 3.

For both composites, as the weight percent  $\text{SiO}_2$  content increases, the velocity is reduced. This trend is not surprising because the thermal properties of  $\text{SiO}_2$  are more insulative than the highly conductive thermal properties of  $\text{Fe}_2\text{O}_3$ .<sup>[11]</sup> For example, the thermal conductivity for  $\text{Fe}_2\text{O}_3$  is 20.0 W/m K and for  $\text{SiO}_2$  is 1.38 W/m K.<sup>[11]</sup> The presence of  $\text{SiO}_2$  hinders flame propagation by behaving as a thermal heat sink and resisting the transport of heat through the mixture, thereby reducing the velocity. Although  $\text{SiO}_2$  contributes to the chemical energy generated (as shown in Equation 4), adding  $\text{SiO}_2$  reduces the overall speed of the reaction by inhibiting thermal transport and reducing the combustion temperature.

A similar decrease in velocity with increasing content of an additive, such as  $\text{Al}_2\text{O}_3$ , has been well established for intermetallic combustion.<sup>[12]</sup> For self-propagating high temperature synthesis (SHS) of metallic alloys,  $\text{Al}_2\text{O}_3$  can be added to a reactant matrix and act as a diluent. This additive offers advantages in the macroscopic behavior of the product alloy.<sup>[12]</sup> For example, small quantities of  $\text{Al}_2\text{O}_3$  (i.e., less than 2 wt %) have been incorporated into a reactant



matrix to enhance the overall strength of the SHS product alloy.<sup>[12c,d]</sup> Only small concentrations will be effective such that flame propagation behavior will not be significantly impacted.<sup>[12c,d]</sup> In this present study, the SiO<sub>2</sub> additive is not acting as a diluent but does possess enough thermal resistance to impede flame propagation. In this way, the SiO<sub>2</sub> additive allows control of the rate of flame propagation through the mixture ratio of SiO<sub>2</sub> to other reactants. This is a distinctly different advantage than that described for SHS, but equally important for tailoring energy release rates.

An interesting aspect of Figure 3 is the relationship between the aerogel oxidizer composite (*Oxidizer A*) and the mechanically mixed oxidizer particles (*Oxidizer B*). When a negligible amount (or no) SiO<sub>2</sub> is within the mixture, *Oxidizer A* produces more than a factor of 4 increase in the velocity over *Oxidizer B* (i.e., 40.5 compared with 8.8 m/s, respectively). This difference is attributed to chemical rather than physical variations between the two oxidizers. For example, Tables 1 and 2 show that the surface area for both oxidizers at 100 % Fe<sub>2</sub>O<sub>3</sub> is roughly the same (44.1 versus 47.8 m<sup>2</sup>/g). Therefore, the key difference in these two mixtures is that *Oxidizer A* is prepared as an aerogel while *Oxidizer B* is discrete particles. The relationship between velocity and synthesis technique shown here is consistent with previous velocity results for the Al/Fe<sub>2</sub>O<sub>3</sub> composite synthesized as an aerogel compared with discrete particles.<sup>[5]</sup> Specifically, Plantier et al.<sup>[5]</sup> showed that Al combined with the Fe<sub>2</sub>O<sub>3</sub> aerogel (prepared in the same manner as this study) resulted in a 10 % increase in velocity when compared to the Al combined with a commercial nm Fe<sub>2</sub>O<sub>3</sub> (also the same nm Fe<sub>2</sub>O<sub>3</sub> used in this study). This was explained by differences in the chemical properties between the aerogel and commercial Fe<sub>2</sub>O<sub>3</sub>. Specifically, the aerogel was shown to be  $\alpha$ -Fe<sub>2</sub>O<sub>3</sub>, the most thermodynamically stable form of Fe<sub>2</sub>O<sub>3</sub>. The commercial particles were shown to exist as amorphous hydrated ferric oxide which

is a poorly crystalline hydrated ferrihydrite phase that possess bonded water (-OH) within its structure. This chemical impurity was shown to inhibit flame propagation. Therefore, in Fig. 3 when 0 % SiO<sub>2</sub> is contained within the mixture, *Thermite B* exhibits a reduced velocity over *Thermite A* because the chemical phase associated with *Oxidizer B* contains an -OH impurity that impedes flame propagation.

The opposite trend, however, is observed for *Thermite A and B* when SiO<sub>2</sub> is included in the oxidizer mixture. With 20 % SiO<sub>2</sub>, *Thermite A* exhibits a 99.4 % reduction in combustion velocity, versus only a 76.3 % reduction in combustion velocity for *Thermite B*. As more SiO<sub>2</sub> is included, further reductions in velocity are observed but the difference in velocity between *Thermite A and B* remained constant. This consistent reduction in velocity with increased SiO<sub>2</sub> content, may result from physical differences that affect the homogeneity of the mixture. Table 1 shows that for Oxidizer A the surface area dramatically increases from 44 to 384 m<sup>2</sup>/g with the addition of SiO<sub>2</sub>. Table 2 shows a marginal increase in surface area for Oxidizer B with added SiO<sub>2</sub>. The increased surface area will enable more contact between the fuel and oxidizer particles improving the homogeneity of the mixture. Even incremental improvements in mixture homogeneity will reduce diffusion distances between fuel and oxidizer particles such that the combustion velocity will increase.

Figure 4 shows still frame images of flame propagation for 0 and 40 wt % SiO<sub>2</sub> content for both sets of composites. For composites containing no SiO<sub>2</sub> (Figure 4a and 4b), the reaction appears to consume all particles, which rise into the air and convectively cool as smoke. More importantly, all of the particles appear to react at the same time. Figure 4b demonstrates the faster progression of the flame front for *Thermite A*.

A different looking reaction for the composites containing 40% SiO<sub>2</sub>, however, can be seen in Figure 4c and 4d. In Figure 4c, many discrete particles can be seen radiating in these frames. The reaction between Al and Fe<sub>2</sub>O<sub>3</sub> may be so exothermic that SiO<sub>2</sub> particles are forced into the air while still radiating and reacting. These radiating particles appear to burn much slower and are apparent even after the plume has disappeared. The physical mixing of discrete particles may facilitate the ejection of the slower reacting SiO<sub>2</sub> from the Al and Fe<sub>2</sub>O<sub>3</sub> reaction zone. This behavior, however, is not apparent in Figure 4d for the 40% SiO<sub>2</sub> *Oxidizer A*. In this case, flame propagation is considerably slower than that shown in Figure 4c, but discrete particles ejected from the flame zone are not apparent. This may result from the sol-gel synthesis of the oxidizer intertwining the Fe<sub>2</sub>O<sub>3</sub> and SiO<sub>2</sub> matrices such that they exist as an interpenetrating network in single particles instead of separate particles.<sup>[13]</sup> In this way, discrete SiO<sub>2</sub> particles cannot be easily ejected from the more exothermic Al + Fe<sub>2</sub>O<sub>3</sub> reaction because SiO<sub>2</sub> does not exist as discrete particles. Overall the propagating reaction is more sluggish because the less exothermic Al + SiO<sub>2</sub> reaction is forced to occur simultaneous with the Al + Fe<sub>2</sub>O<sub>3</sub> reaction, thus reducing the overall velocity. As more SiO<sub>2</sub> is added to the oxidizer matrix, a consistent reduction in velocity is observed. This finding suggests that there may be a larger amount of unreacted material in *Thermite B*; although *Thermite A* propagates slower, more reactants are consumed and the combustion process is more complete.

This study examined the combustion velocity of two ternary composites both consisting of Al/Fe<sub>2</sub>O<sub>3</sub>/SiO<sub>2</sub> but mixed using two different preparation methods. The first was chemically combined oxidizers using sol-gel processing combined with nano-Al particles (*Thermite A*). The second physically mixed discrete nano-scale particles together in solution using sonic waves (*Thermite B*). The inclusion of SiO<sub>2</sub> was used as a means to control the combustion velocity.

Results show that  $\text{SiO}_2$  acts as a heat sink and retards flame propagation reducing the combustion velocity. An interesting finding from this study is determined from examining the flame propagation behavior as a function of preparation method. The aerogel composites are “intertwined” such that a more complete reaction between the Al fuel and both oxidizers is forced to occur. For the physically mixed discrete particles, the less exothermic  $\text{SiO}_2$  particles are ejected from the more exothermic  $\text{Al} + \text{Fe}_2\text{O}_3$  reaction zone prior to their complete reaction. This behavior suggests that the sol-gel processing of a composite allows for increased homogeneity between reactants and products which promotes more complete combustion. Finally, the combustion velocity can be controlled by the amount of  $\text{SiO}_2$  added to the composite, and the manner by which the  $\text{SiO}_2$  is mixed into the oxidizing phase.

## *Experimental*

### *Aerogel Synthesis*

Aerogel oxidizers were prepared via a previously described sol-gel technique followed by supercritical processing in a Polaron™ supercritical point dryer.<sup>[10c]</sup> All aerogels were subsequently heated at 10 °C/min to 410 °C and held for 4 hours. Following calcination, the oven was switched off and the aerogel oxidizers were allowed to cool to room temperature overnight.

### *Sample Preparation*

The energetic composites were prepared by physically mixing commercially obtained fuel and oxidizer particles or by physically mixing fuel and the aerogel oxidizers. The fuel particles were 80 nm average diameter aluminum ( Nanotechnologies Inc.) passivated with an alumina ( $\text{Al}_2\text{O}_3$ ) shell that is roughly 4 nm thick and encapsulates the core Al particle. Based on

thermal analysis, the manufacturer determined that this powder has an active Al content of 81 %. Active Al is defined as the portion of powder not in the form of  $\text{Al}_2\text{O}_3$ . The commercial oxidizer powders were submicron  $\text{SiO}_2$  (Alfa Aesar) and 3 nm diameter  $\text{Fe}_2\text{O}_3$  (Sigma-Aldrich). The purity of both of the oxidizer chemicals was reported to be greater than 99 % and assumed to be 100 % pure for our stoichiometric calculations.

Mixing was accomplished by suspending the relevant amounts of Al,  $\text{Fe}_2\text{O}_3$ , and  $\text{SiO}_2$  (set 1) or Al and aerogel  $\text{Fe}_2\text{O}_3/\text{SiO}_2$  (set 2) in 60 mL of hexane. The mixtures were sonicated using a Misonix Sonicator 3000 sonic wand and the hexane was allowed to evaporate on a hot plate at a temperature of  $\sim 80^\circ\text{C}$ . Once the powders were dry, a homogeneous mixture was ready for further experimentation.

#### *Combustion Velocity Measurements*

Combustion velocities were measured using a Phantom IV high-speed camera (*Vision Research*) that records images up to 32,000 frames per second (fps). The camera records visible emission at 128 x 32 pixels and uses a Nikon AF Nikkor 28 mm 1:2.8 D lens. The camera interfaces with a computer which transfers the recorded file from the camera and has a data analysis program from *Vision Research* that measures velocity. For each test, 150 mg of thermite powder mixture was used. Ignition was achieved using a spark ignition system for loose powders in a 0.3175 cm square channel 10 cm in length cut into a transparent acrylic block, as shown in Figure 2. All combustion velocities were measured in an open air environment.

#### *Physical Characterization*

Surface area measurements and pore size distributions of the aerogel oxidizers were determined by nitrogen adsorption/desorption using a Micromeritics ASAP2000 gas adsorption analyzer. Surface areas were calculated from a 5 point data analysis between 0.05 and 0.2

relative pressure at 77 K using BET (Brauner, Emmett, and Teller) theory. Pore volumes were determined from  $N_2(g)$  desorption isotherms using BJH (Barrett-Joyner-Halenda) theory. Chemical analysis was performed on the aerogel-oxidizer samples by Galbraith Laboratories Inc. (Knoxville, TN). The levels of carbon and hydrogen were measured simultaneously based on the concentration liberated during combustion using an IR or thermal conductivity detector. Concentration levels of  $CO_2$  and  $H_2O$  were also determined using an IR detector. Levels of iron and silicon were measured by dissolving the solid in a mineral acid and using an Inductively Coupled Plasma - Optical Emission Spectrophotometer (ICP-OES). The surface areas and purity of the aerogel-oxidizers are reported in Table 1.

*Submitted to Advanced Materials January, 2004.*

## References

- [1] W. C. Danen, J. A. Martin, *US Patent No. 5 266 132*, **1993**.
- [2] S. H. Kim, M. R. Zachariah, *Adv. Mater.* **2004**, *16*, 1821.
- [3] T. M. Tillotson, A. E. Gash, R. L. Simpson, L. W. Hrubesh, J. H. Satcher Jr., J. F. Poco, *J. Non-Cryst. Solids* **2001**, *285*, 338.
- [4] a) A. E. Gash, T. M. Tillotson, J. H. Satcher Jr., J. F. Poco, L. W. Hrubesh, R. L. Simpson, *Chem. Mater.* **2001**, *13*, 999-1007. b) A. E. Gash, T. M. Tillotson, J. H. Satcher Jr., L. W. Hrubesh, R. L. Simpson, *J Non-Cryst. Solids* **2001**, *285*, 22-28. c) B. J. Clapsaddle, A. E. Gash, J. H. Satcher Jr., R. L. Simpson, *J. Non-Cryst. Solids* **2003**, *331*, 190. d) B. J. Clapsaddle, D. W. Sprehn, A. E. Gash, J. H. Satcher Jr., R. L. Simpson, *J. Non-Cryst. Solids* **2004**, *350*, 173.
- [5] Plantier, K. B., Pantoya, M. L., Gash, A. E., *Combustion and Flame* **2005**, *13*(7), 1-11.
- [6] A. E. Gash, J. H. Satcher Jr., R. L. Simpson Jr., B. J. Clapsaddle, "Nanostructured Energetic Materials with Sol-gel Methods", *Mat. Res. Soc. Symp. Proc.*, **2004**, *800*, AA2.2.1
- [7] B. J. Clapsaddle, L. Zhao, A. E. Gash, J. H. Satcher Jr., K. J. Shea, M. L. Pantoya, R. L. Simpson, "Synthesis and Characterization of Mixed Metal Oxide Nanocomposite Energetic Materials", *Mat. Res. Soc. Symp. Proc.*, **2004**, *800*, AA2.7.1
- [8] Granier, J. J. and Pantoya, M. L., *Combustion and Flame* **2004**, *138*, 373-383.
- [9] Fischer, S. H. and Grubelich, M. C., "Theoretical Energy Release of Thermites, Intermetallics, and Combustible Metals," 24<sup>th</sup> International Pyrotechnics Seminar, Monterey, CA **1998** (also a Sandia Technical Report number SAND98-1176C)
- [10] Bockmon, B. S., Pantoya, M. L., Son, S. F., Asay, B. W., Mang, J. T., "Combustion Velocities and Propagation Mechanisms of Meta-stable Intermolecular Composites," Submitted to the *Journal of Applied Physics*, December, 2004.

- [11] Weast, R. C. (Editor-in-Chief), CRC Handbook of Chemistry and Physics 64<sup>th</sup> Ed., CRC Press, Inc, Boca Raton, FL (1984).
- [12] a) Munir, Z. A., “Reaction Synthesis Processes: Mechanisms and Characteristics,” *Metallurgical Transactions A*, v. 23A, pp. 7-13 (1992)). b) Varma, A., C.R. Kackelmyer, and A.S. Rogachev, “Mechanistic Studies in the Combustion Synthesis of Aluminides and Silicides.” *International Journal of Self-Propagating High-Temperature Synthesis*, v. 5, n. 1. (1996). c) Mukasyan, A. S., Rogachev, A. S., Varma, A., “Mechanisms of Reaction Wave Propagation During Combustion Synthesis of Advanced Materials,” *Chemical Engineering Science*, v 54, pp. 3357-3367 (1999). d) Granier, J. J., Plantier, K. B., and Pantoya, M. L. “The Role of the Al<sub>2</sub>O<sub>3</sub> Passivation Shell Surrounding Nano-Aluminum Particles in the Combustion Synthesis of NiAl,” *Journal of Materials Science* vol. 39 pp. 1-11 (2004).
- [13] L. Zhao, B. J. Clapsaddle, J. H. Satcher Jr., K. J. Shea, *submitted to Chem. Mater.*, **2004**.



## Figure Captions

- Figure 1. Schematic diagram illustrating bimodal oxidizer mixture ratios for A. sol-gel synthesized oxidizer composites (*Oxidizer A*); and, B. commercial powders physically mixed (*Oxidizer B*).
- Figure 2. Photograph of open channel apparatus used for measuring combustion velocity.
- Figure 3. Combustion velocity as a function of  $\text{SiO}_2$  content on a logarithmic velocity scale. *Thermite A* corresponds to the Al combined with sol-gel synthesized aerogel  $\text{Fe}_2\text{O}_3/\text{SiO}_2$  composite and *Thermite B* corresponds to the Al combined with discrete nm particles of  $\text{Fe}_2\text{O}_3$  and  $\text{SiO}_2$ .
- Figure 4. Still frame images from high speed photographic data for A. 0 % wt  $\text{SiO}_2$  Thermite B; B. 0 % wt  $\text{SiO}_2$  Thermite A; C. 40 % wt  $\text{SiO}_2$  Thermite B; and, D. 40 % wt  $\text{SiO}_2$  Thermite A.

Table 1. Chemical<sup>a</sup> and physical analysis of sol-gel prepared Fe<sub>2</sub>O<sub>3</sub>/SiO<sub>2</sub> (*Oxidizer A*).

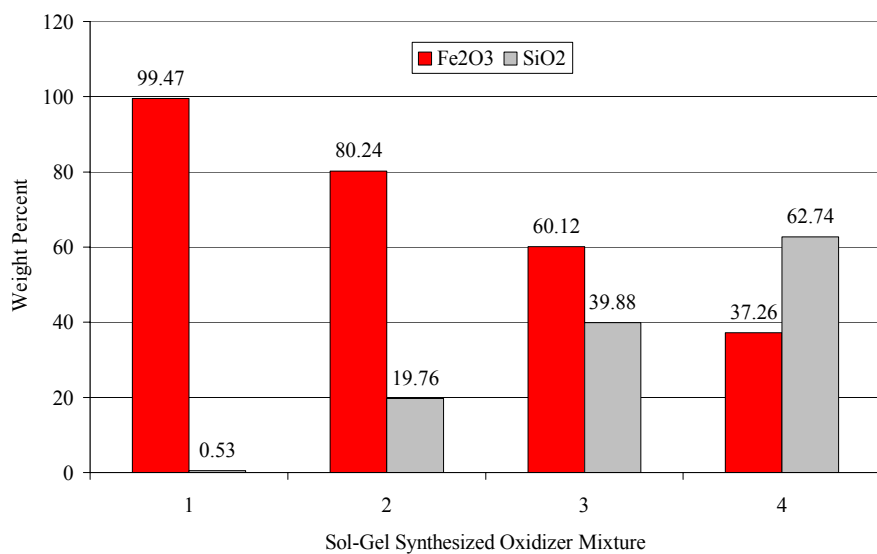
<b>oxidizer</b>	<b>%Fe</b>	<b>%Si</b>	<b>%C</b>	<b>%H</b>	<b>%Fe<sub>2</sub>O<sub>3</sub><sup>a</sup></b>	<b>%SiO<sub>2</sub></b>	<b>surf. area (m<sup>2</sup>/g)</b>	<b>pore volume (cm<sup>3</sup>/g)</b>
100/0	64.1	0.23	< 0.5	< 0.5	99.5	0.5	44.1	0.32
80/20	53.5	8.81	< 0.5	0.9	80.2	19.8	384	3.74
60/40	38.2	16.9	< 0.5	1.1	60.1	39.9	350	1.54
40/60	23.9	26.8	< 0.5	1.24	37.3	62.7	342	1.21

a. All chemical compositions are reported as weight percents. The small amounts of carbon and hydrogen present were not taken into consideration for calculation of % Fe<sub>2</sub>O<sub>3</sub> and % SiO<sub>2</sub>.

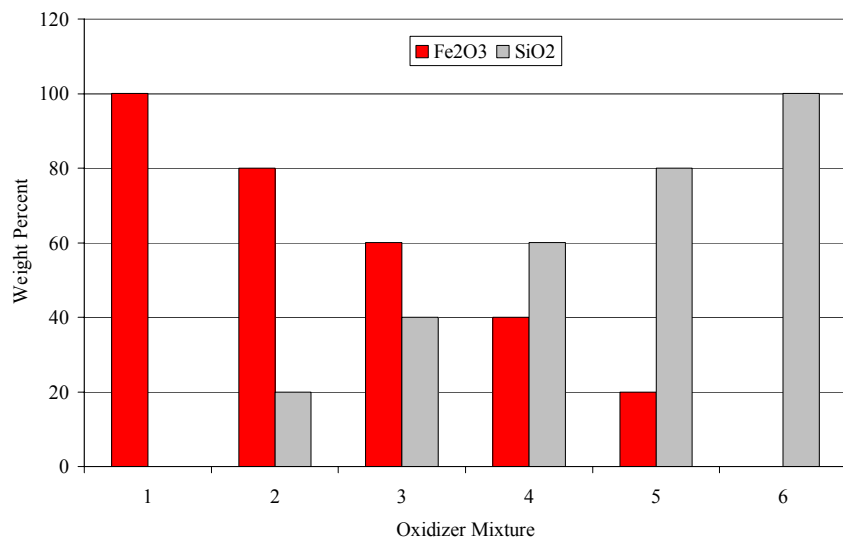
Table 2. Surface area and pore volumes for discrete particles Fe<sub>2</sub>O<sub>3</sub> and SiO<sub>2</sub> mechanically mixed (*Oxidizer B*).

<b>oxidizer composition<sup>a</sup></b>	<b>surface area (m<sup>2</sup>/g)</b>	<b>pore volume (cm<sup>3</sup>/g)</b>
100% Fe <sub>2</sub> O <sub>3</sub>	47.8	0.23
80% Fe <sub>2</sub> O <sub>3</sub> /20% SiO <sub>2</sub>	54.9	0.31
60% Fe <sub>2</sub> O <sub>3</sub> /40% SiO <sub>2</sub>	66.9	0.32
40% Fe <sub>2</sub> O <sub>3</sub> /60% SiO <sub>2</sub>	76.5	0.32
20% Fe <sub>2</sub> O <sub>3</sub> /80% SiO <sub>2</sub>	—	—
100% SiO <sub>2</sub>	93.4	0.28

<sup>a</sup>. Mixtures are reported as weight percents.



A.



B.

Figure 1. Schematic diagram illustrating bimodal oxidizer mixture ratios for A. sol-gel synthesized oxidizer composites (*Oxidizer A*); and, B. commercial powders physically mixed (*Oxidizer B*).

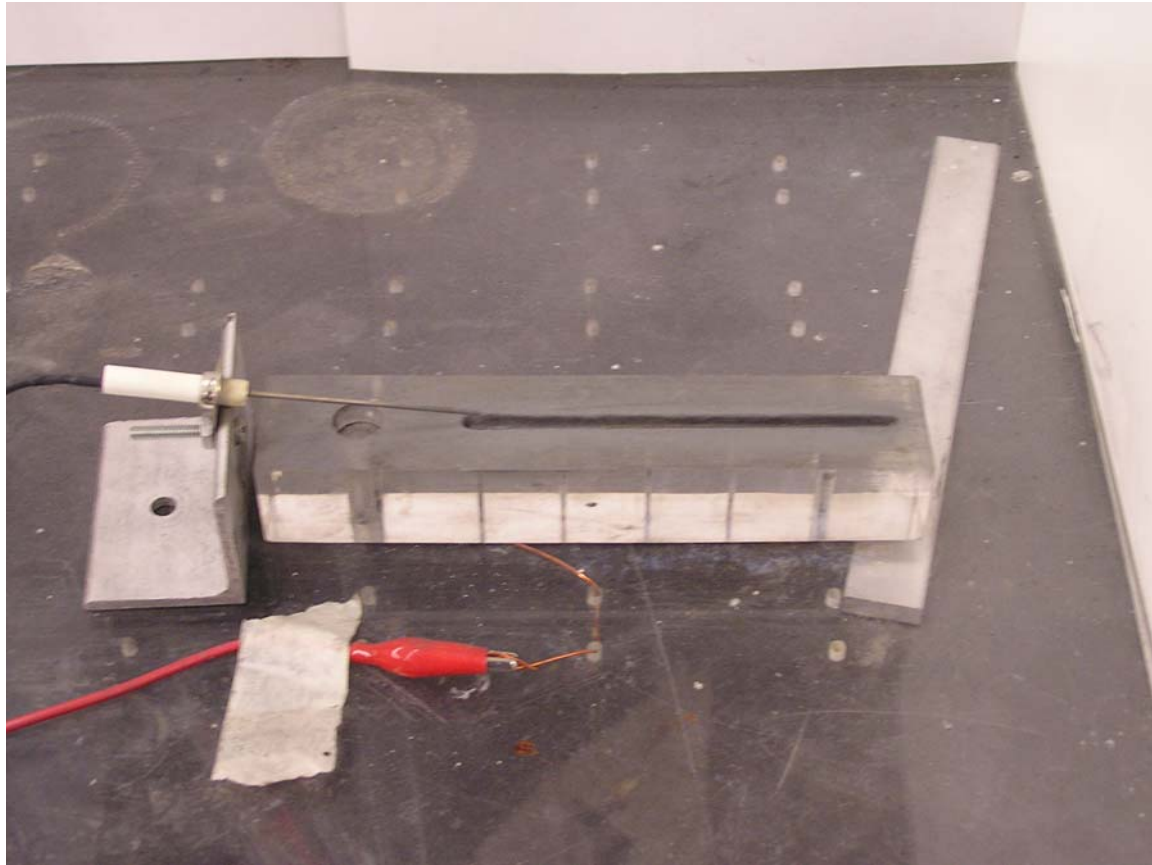


Figure 2. Photograph of open channel apparatus used for measuring combustion velocity.

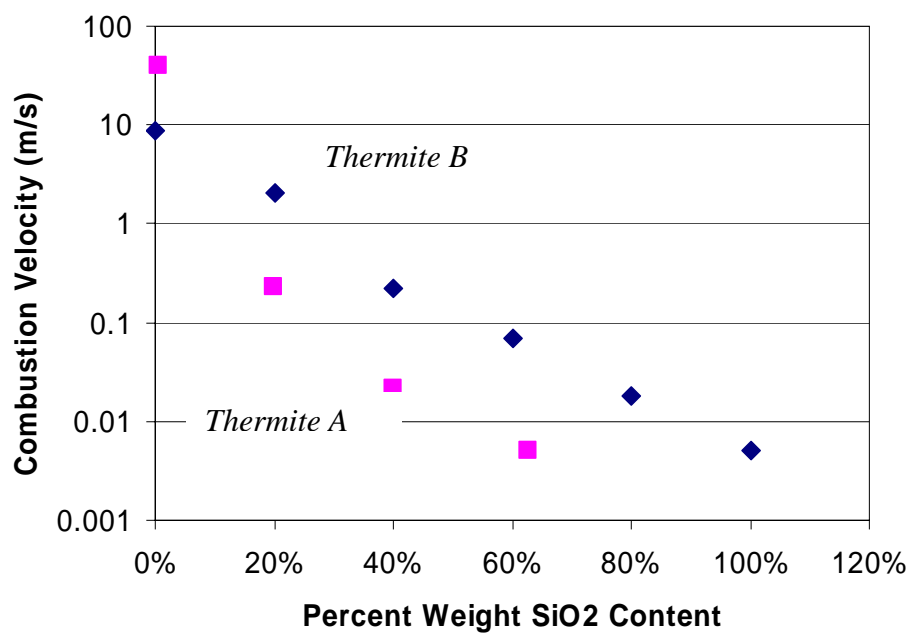


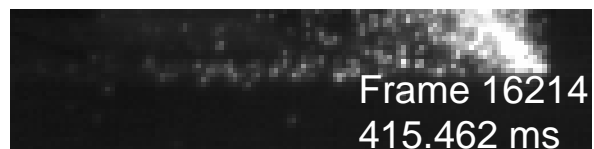
Figure 3. Combustion velocity as a function of SiO<sub>2</sub> content on a logarithmic velocity scale. *Thermite A* corresponds to the Al combined with sol-gel synthesized aerogel Fe<sub>2</sub>O<sub>3</sub>/SiO<sub>2</sub> composite and *Thermite B* corresponds to the Al combined with discrete nm particles of Fe<sub>2</sub>O<sub>3</sub> and SiO<sub>2</sub>.

Thermite B: 0.00% wt.  $\text{SiO}_2$



A.

Thermite B: 40.0% wt.  $\text{SiO}_2$



C.

Thermite A: 0.53% wt.  $\text{SiO}_2$



B

Thermite A: 39.9% wt.  $\text{SiO}_2$



D.

Figure 4. Still frame images from high speed photographic data for A. 0 % wt  $\text{SiO}_2$  Thermite B; B. 0 % wt  $\text{SiO}_2$  Thermite A; C. 40 % wt  $\text{SiO}_2$  Thermite B; and, D. 40 % wt  $\text{SiO}_2$  Thermite A.